Chapter 3

Non-parametric Models for Magneto-Rheological Dampers

The primary purpose of this chapter is to present an approach for developing non-parametric models for magneto-rheological (MR) dampers. Upon describing the approach adopted here, a non-parametric model for a commercial magneto-rheological damper is developed, and is compared with a parametric model from an earlier study. The results show that the proposed non-parametric model can more effectively represent the nonlinear characteristics of MR dampers, and more readily lends itself to adaptive control techniques for MR systems.

3.1 Magneto-Rheological Damper Models

There exist two general methods for modeling devices, such as MR dampers. One is the parametric modeling technique that characterizes the device as a collection of springs, dampers, and other physical elements. The second method, called non-parametric modeling, employs analytical expressions to describe the characteristics of the modeled devices. In this section, we summarize some of the significant parametric and non-parametric modeling results, developed for ER and MR dampers.

Both ER and MR devices have similar nonlinearities such as hysteresis and saturation. Thus, their modeling techniques are similar. A group of earlier studies used the non-parametric models to describe ER fluid and devices. Ehrgott and Marsi [61] used the Tchebycheff function to model ER fluid. Their model is quite complicated, as it requires a large number of higher terms in order to maintain sufficient accuracy. McClamroch and Gavin [62] and Hsu and Meyer [63] used the trigonometric functions to describe hysteresis but their models could not be used to capture the saturation of the damping force in the high velocity region for MR or ER devices.

A number of other studies have addressed the parametric modeling of magneto-rheological (MR) and electro-rheological (ER) dampers. Parametric models refer to those

models in which the characteristics of the dampers are represented by a series of linear and nonlinear elements with defined parameters, such as springs and dampers. The Bingham viscoelastic-plastic model, described by Shames and Cozzarelli [64], was used in the modeling studies on ER fluid and devices such as Kamath and Wereley [65]. In another study by Kamath and Wereley [66], they used different linear shear flow mechanisms to describe pre-yield and post-yield regions of ER devices. A model was built as a nonlinear combination of both regional models. The parameters were optimized for each field strength, and polynomial functions were used to approximate the curve for each parameter to achieve a comprehensive analytical model.

In another study, Spencer et al [67, 68] provide a parametric model for MR dampers, as shown in Fig. 3, based on the extension of the Bouc-wen model [69]. The Bouc-wen model is derived from a Markov-vector formulation to model nonlinear hysteretic systems.

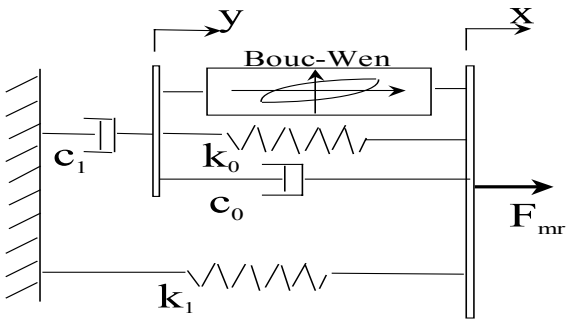

Figure 3.1 Configuration of the Parametric MR Damper Model

From the model in Fig. 3.1, the MR damper force can be predicted according to

$$\begin{cases} \dot{z} = -\gamma |\dot{x}-\dot{y}||z|z|^{n-1} - \beta(\dot{x}-\dot{y})|z|^{n} + A(\dot{x}-\dot{y}) \\ \dot{y} = \dfrac{1}{c_0 + c_1}\{\alpha z + c_0\dot{x} + k_0(x-y)\} \\ F_{mr} = c_1\dot{y} + k_1(x-x_0) \end{cases} \tag{3.1}$$

The parameters β, γ and A in the Bouc-Wen model are used to control the linearity in the unloading and the smoothness of the transition from the pre-yield to the post-yield region. The accumulator stiffness is represented by k_1 and the viscous damping observed at larger

velocities is represented by c_0. A dashpot, represented by c_1, is included in the model to produce the roll-off at low velocities, k_0 is used to control the stiffness at larger velocities, and x_0 is the initial displacement of spring k_1 associated with the nominal damper due to the accumulator. In addition, z is a revolutionary variable, and F_{mr} is the predicted damping force.

The damping constants c_0 and c_1 depend on the electrical current applied to the MR damper, and in the Spencer model they are formulated as

$$\begin{cases} \dot{u} = -\eta(u - v) \\ \alpha = \alpha(u) = \alpha_a + \alpha_b u \\ c_1 = c(u) = c_{1a} + c_{1b} u \\ c_0 = c(u) = c_{0a} + c_{0b} u \end{cases} \tag{3.2}$$

The variable u is the current applied to the damper through a voltage-to-current converter with a time constant η. The variable v is the voltage applied to the converter.

Although the parametric models mentioned above effectively characterize MR dampers in terms of the Bouc-Wen model, they are often difficult to solve numerically. This is mainly due to the sharp transition nonlinearity that commonly exists in such models in order to represent the nonlinear behavior of the dampers. Our experience shows that such models cannot be included in the real-time controllers or in the controller design simulations; without making special provisions for dealing with the stiff differential equations, such as using very fast micro-controllers. Furthermore, parametric models often do not include the magnetic field saturation that is inherent in MR dampers. The representation of the magnetic field saturation is often crucial in accurately using the MR damper model for design analysis and control purposes. Therefore, alternative models are necessary to better represent the characteristics of MR dampers with quick numerical solution.

This chapter will discuss a non-parametric model for MR dampers, and devices that behave similar to them, as an alternative to the parametric models that currently exist. The development of the model, along with the logic that is used in configuring it, is presented first. Our approach involves

- evaluating the experimental force characteristics of MR dampers,
- combining a series of equations that can capture various trends of the experimental data, and
- using an optimization routine to fit the selected equations to the data through selecting various coefficients in the equations.

Each aspect of this approach is described in details in the following sections. Finally, the results of the model are compared with the experimental test data for an MR damper and the parametric model suggested by Spencer, et al.

3.2 Experimental Data Analysis

The data used for identifying the force-velocity characteristics of the dampers and calibrating our models were provided by Lord Corporation, Cary, NC. The data included the force trace (i.e., force versus time), force-velocity, and force-displacement characteristics of a damper that was designed for seat suspension applications. As shown in Fig. 3.2, each plot includes six selected curves that correspond to the damper behavior as the electrical current supplied to the damper is changed from zero to two Amperes, in increments of 0.25 Ampere. All data are recorded as the damper rod is displaced +/- 0.5 inch, relative to the body of the damper, at 2.5 Hz.

As the plots in Fig. 3.2 show, for zero Amperes, the MR damper exhibits a nearly Newtonian behavior, i.e., linear viscoelastic relationship between damping force and velocity in Fig. 3.2b, and an elliptic curve in the damping force against displacement as in Fig. 3.2c. At the higher current settings, the MR damper appears to exhibit a Non-Newtonian or quasi-viscous behavior.

In order to build a relatively accurate model for MR dampers, we determined that it is necessary to evaluate different aspects of damper behaviors separately and use appropriate functions to describe each aspect. For instance, Figure 3.2a shows that the period of damping force directly corresponds to the excitation frequency and the curves resemble sine or square waves. Therefore, we can conclude that the damper force frequency is directly dependent on the excitation frequency. As such, the model must be a function that preserves the velocity period in the time domain. The hyperbolic function TANH can readily show such a trend if the exponent is a function of velocity. Nayfeh [70] derived the solution to boundary layer problems as a hyperbolic function. The use of the function TANH is advocated here to describe the characteristics of the transition from pre-yield to post-yield rheological domain, which exists in MR and ER fluids and their devices. Additionally, as shown in Fig. 3.2b, the force-velocity curves exhibit a short bend that corresponds to the transition of the MR fluid from pre-yield to post-yield region. The transition commonly occurs at the same velocity, but at different force levels, for different currents applied to the damper. The function TANH can mimic the transition in phase with the velocity if the parameters are properly chosen. Therefore, it can be concluded that TANH or its derivatives could be used as a backbone shape function to not only preserve the frequency but also create the transitions shown in Figs. 3.2a and 3.2b.

Figure 3.2d shows the relationship between damping level and electrical current to the damper. For MR dampers, the damping level depends on the strength of the applied magnetic field. The damping level shows the saturation phenomenon caused by the magnetic field saturation with the increased electrical current to the damper. The damper force saturation is indicated by the slope of the maximum force-current curve in Fig.

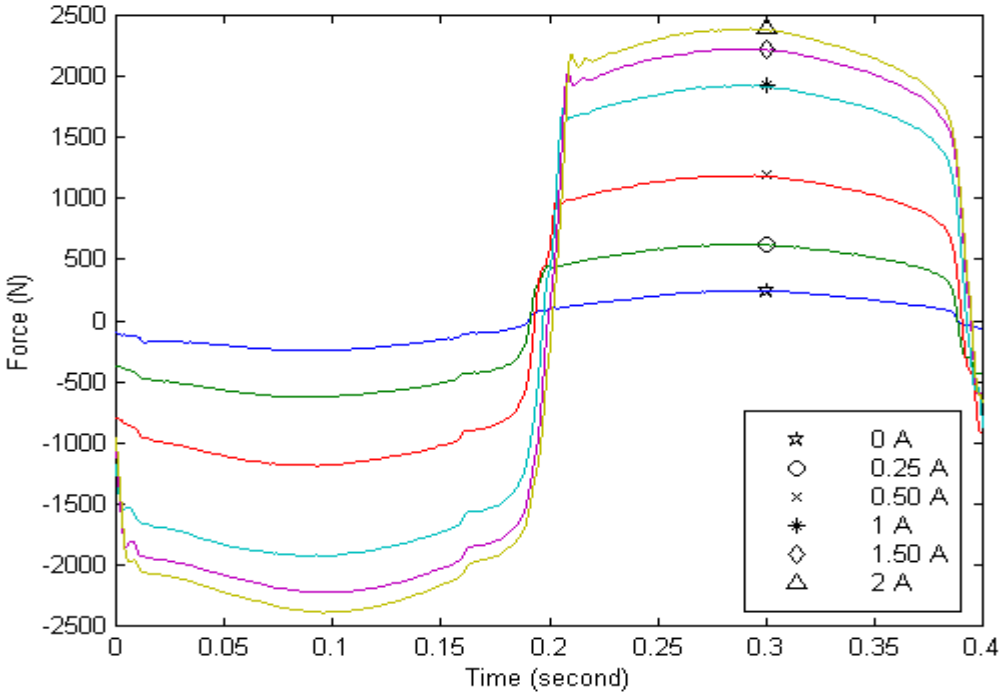

(a)

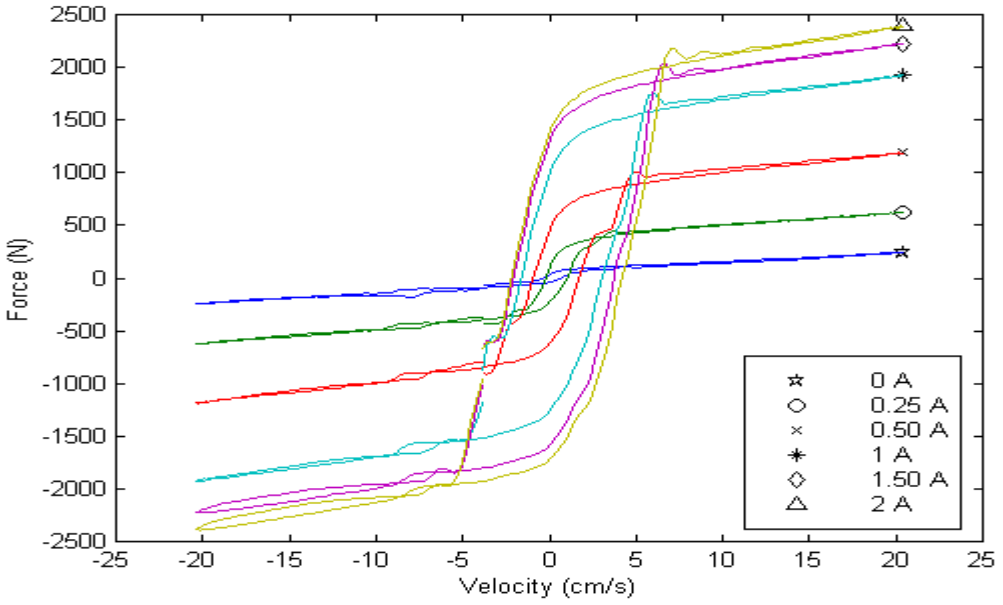

(b)

Figure 3.2 Presentation of Experimental Data of MR Damper:
(a) Time Track; (b) Force Versus Velocity

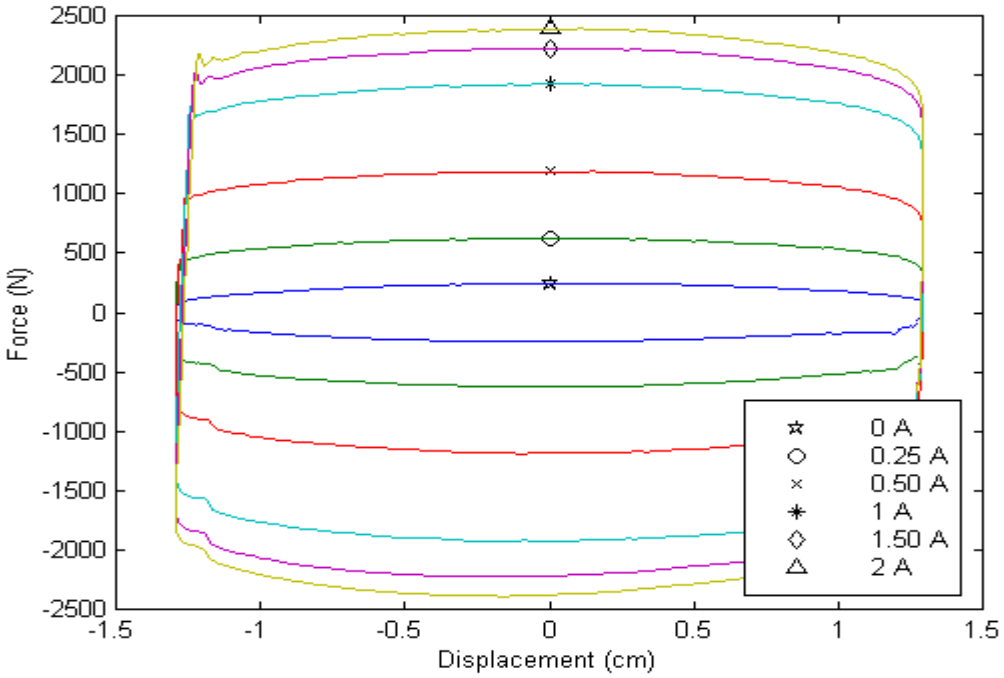

(c)

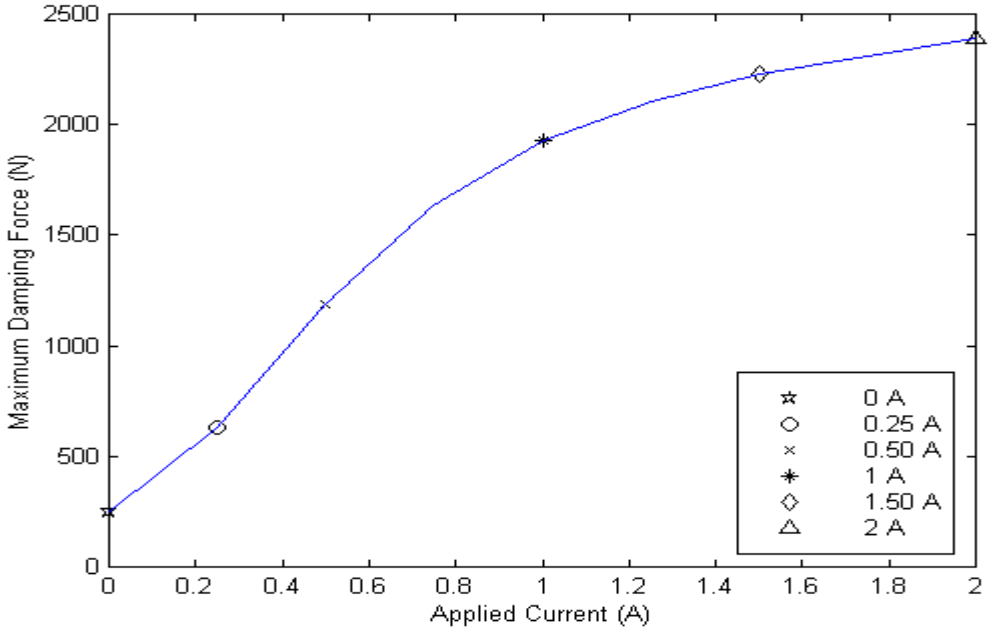

(d)

Figure 3.2 Presentation of Experimental Data of MR Damper:
(c) Force Versus Displacement; (d) Maximum Force Versus Current

3.2d. The slope of the curve flattens at larger currents, indicating the occurrence of damping force saturation. In order to capture such a trend, a polynomial function is used to depict the relationship between damping level and current.

Further, it is observed in Figs. 3.2b and 3.2c that hysteresis loops exist in the MR damper. Usually hysteresis means that there exists a phase lag between the concerned variables, in this case the damping force and velocity. A convenient way to model the phase-lag relationship between damping force and velocity is to use a first-order filter. It is worth noting that the hysteresis width in Fig. 3.2b depends on the applied current. Therefore, the coefficients of the first order filter must be functions of the current.

From the above discussion on the experimental data, a non-parametric model is proposed in the next section to capture the complicated nonlinearities inherent in MR dampers.

3.3 Non-Parametric Model Development

Based on the discussion in the previous section, four mathematical functions are proposed to capture the nonlinearities of MR dampers. The model is composed of the following functions:

1. A Polynomial (Amplitude) Function: A function such as

$$A_{mr}(I) = \sum_{i=0}^{n} a_i I^i \tag{3.3}$$

is used to describe the maximum damping force as a function of the applied current I applied to the MR damper. In Eq. (3.3), A_{mr} is the maximum damping force, a_i are the polynomial coefficients with appropriate units, and n is the order of the polynomial.

2. A Shape Function: A modified hyperbolic function (TANH), such as

$$S_b(V) = \frac{(b_0 + b_1|V - V_0|)^{b_2(V-V_0)} - (b_0 + b_1|V - V_0|)^{-b_2(V-V_0)}}{b_0{}^{b_2(V-V_0)} + b_0{}^{-b_2(V-V_0)}} \tag{3.4}$$

is used to preserve the frequency correlation between the damper force and relative velocity across the damper, and also represent the bilinear behavior of the force-velocity curve. In Eq. (3.4), b_i, i=0-2, are positive constants, V is the velocity across the MR damper, and V_0 is a constant value. Combining Eqs. (3.3) and (3.4) yields the damper force as a function of damper current and relative velocity, i.e.,

$$F_s = A_{mr}(I)S_b(V) \tag{3.5}$$

3. A Delay Function: A first order filter is used to create the hysteresis loop. In its state space form, this filter can be formulated as

$$\begin{cases} \dot{x} = -(h_0 + h_1 I + h_2 I^2)x + h_3 F_s \\ F_h = (h_0 + h_1 I + h_2 I^2)x + h_4 F_s \end{cases} \tag{3.6}$$

where x is a state variable of the filter, h_i, i=0-2, are constants and h_i, i=3-4, are constants or functions of current, and I is the current applied to the MR damper, as defined earlier in Eq. (3.3). F_h combines the damping force F_s shown earlier in Eq. (3.5) and the hysteresis function. It is worth noting that

$$h_0 + h_1 I + h_2 I^2 > 0$$

must be satisfied in order for Eq. (3.6) to be stable (i.e., have a decaying solution).

4. Offset Function: In some cases, the damping force is not centered at zero because of the effect of the gas-charged accumulator in the damper. Therefore, it is necessary to include a force bias in the model, such as

$$F_{mr} = F_h + F_{bias} \tag{3.7}$$

where F_{bias} represents the non-zero centered damping force and F_{mr} is the damping force of the MR damper.

The combination of the four functions mentioned above provides the non-parametric model, as presented in Eqs. (3.3) to (3.7). Next, we will discuss the selection of the model parameters and evaluate the model accuracy by comparing the model results with experimental data.

3.4 Model Parameter Estimation

The parameters in the proposed non-parametric model are estimated by using the data shown in Fig. 3.2 for applied currents of 0 to 2 Amperes. An optimization process is used to minimize the error between the measured damping force and the force predicted by the model, according to the objective function

$$J = \sum_{k=1}^{N} \{F_{mr}(k) - F_{ex}(k)\}^2 \tag{3.8}$$

where F_{ex} is the experimentally measured force, F_{mr} is the force calculated from the model, and N is the total number of the experimental data from 0 to 2 Amperes.

A constrained optimization routine is used to select the model parameters that minimize the objective function in Eq. (3.8) and satisfy the constraints which specify the selection region for the model parameters, according to the flow chart in Fig. 3.3. Because of limits on the feasible region for the parameters, the optimizer can make well-informed decisions regarding directions of search and step length. Furthermore, appropriate initial values for optimal selection of the model parameters are necessary to ensure that the optimization process converges fast and properly, because nonlinear optimization problems are highly sensitive to the initial values of the parameters.

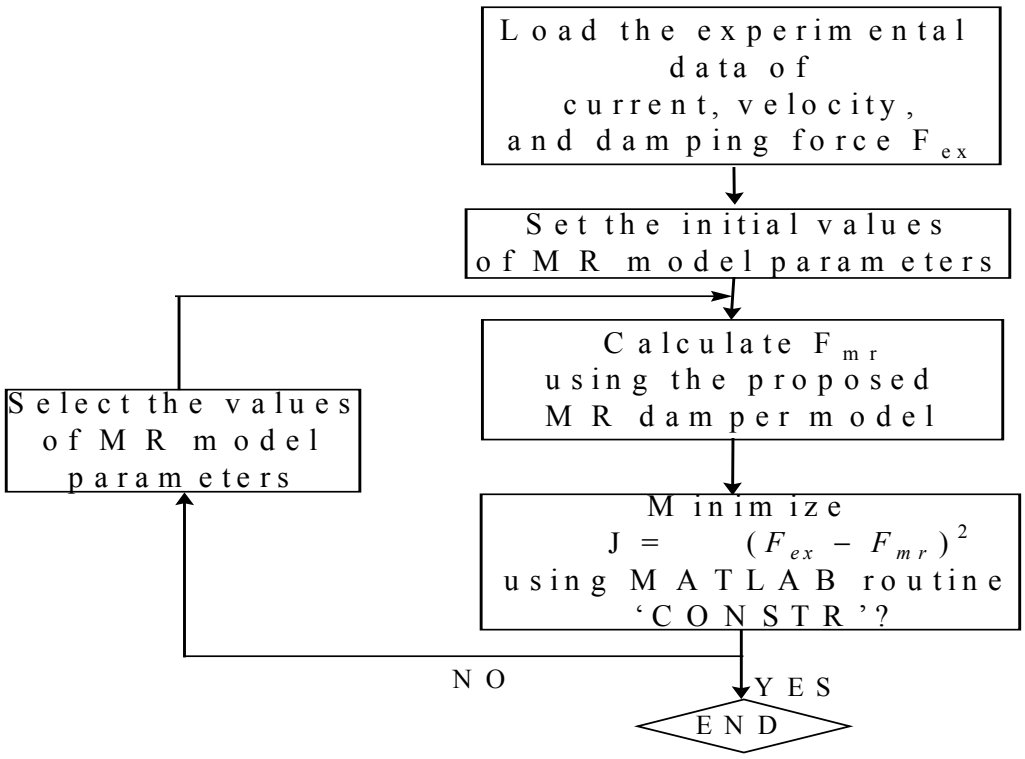

Figure 3.3 Flow Chart of MATLAB Codes to Select Values of MR Model Parameters

As far as initial values are concerned, they were determined by trial and error. For example, the polynomial coefficients a_i, i=0-4, were determined initially by using the least-mean-square method according to the maximum force-current data. Next, we ran the program a few more times to decide the initial values of the other parameters. Our experience showed that such a procedure provides effective initial values for the constrained optimization routine CONSTR in MATLAB that was used for this purpose.

All parameters were constrained within a range that was equal to +/- two times the initial values for the parameters. For instance, a parameter with an initial value of +1 was constrained to a range of –1 to +3. We determined this range empirically, as our experience showed that it is large enough to allow convergence to acceptable solutions, and yet small enough to avoid numerical stability. For some models, we ran the optimization routine multiple times to check the effect of different parameter constraints on the solution.

The model parameters are as shown in Table 3.1, for the MR damper that we selected for this study. It is worth noting that if one chooses a different damper, a different set of data, or a different optimization routine, the parameters in Table 3.1 may significantly change.

Table 3.1 Optimal Values of the Proposed Model

Parameter	Value	Parameter	Value	Parameter	Value
A_0	164.8	b_0	5.8646	h_2	566.0
A_1	1316.5	b_1	0.0060	h_3	1
A_2	1407.8	b_2	0.2536	h_4	0
A_3	-1562.8	h_0	299.7733	V_0	0.6248
A_4	388.8	h_1	-210.320	F_{bias}	0

3.5 Comparison with a Parametric Model

In order to evaluate the effectiveness of the non-parametric model developed in the previous section, we compared it with the experimental data and the parametric model that was developed in [67, 68] for nearly the same MR damper as the one we tested. Therefore, a comparison between the two models is justified. The parameters selected for our non-parametric model are according to Table 3.1, whereas the parametric model parameters are as documented in [67, 68].

In comparing the non-parametric model to the mentioned parametric model, some of the immediate observations that we made were

1. Increased numerical efficiency,
2. Better representation of force saturation, and
3. More accuracy for broader operating conditions.

3.5.1 Numerical Efficiency

Our experience with the parametric and non-parametric models proved that one is able to solve the non-parametric models described by Eqs. 3.3 to 3.8, much faster than the Eqs. 3.1 and 3.2 for a parametric model. This may be apparent to the naked eye, as one set of equations involves stiff differential equations and another does not. As such one is able to integrate the non-parametric models with much larger step sizes than the parametric model. In our case, we choose a step size of 10^{-5} second for the parametric model and 10^{-2} for the non-parametric model, a difference of 1000 times.

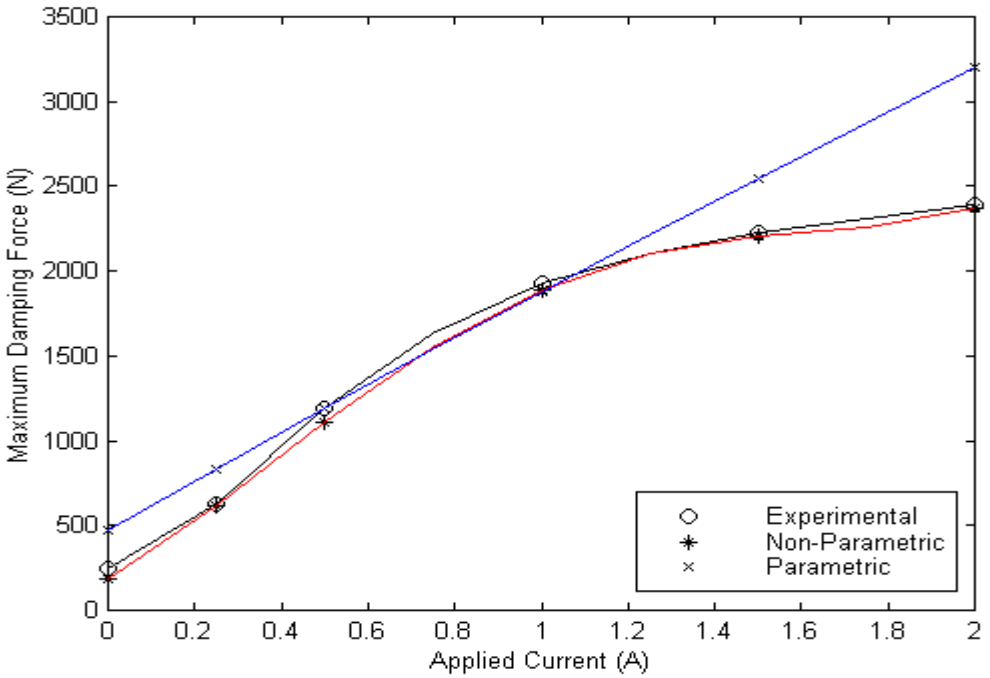

Figure 3.4 Prediction of Damper Force Saturation by Parametric and Non-Parametric MR Damper Models

3.5.2 Force Saturation Representation

Figure 3.4 shows that the non-parametric model can better capture the saturation phenomenon inherent in the MR dampers. The non-parametric model much more closely follows the experimental data than the parametric model that exhibits a linear curve for maximum force vs. current. This is mainly due to the fact that the non-parametric model

explicitly accounts for the damper force saturation, whereas the parametric model lacks such a mechanism.

3.5.3 Accuracy across the Operating Condition

Figures 3.5 to 3.7 show the force trace (i.e. force vs. time), force-velocity, and force-displacement characteristics of the dampers for six different applied currents. Each plot demonstrates that the non-parametric model is able to more closely predict the experimental data than the parametric model, for all current levels. Two factors mainly contribute to this phenomenon. Firstly, the parameters for the non-parametric models are selected such that the model fits the experimental data. Although the same is true for the parametric model, it is configured such that the data fit is specific to a single current, and for other currents the model may not predict the experimental data with the same accuracy. Secondly, as mentioned earlier, the parametric model does not account for the damper force saturation, and as such it deviates from the experimental data when saturation occurs, for example at higher currents.

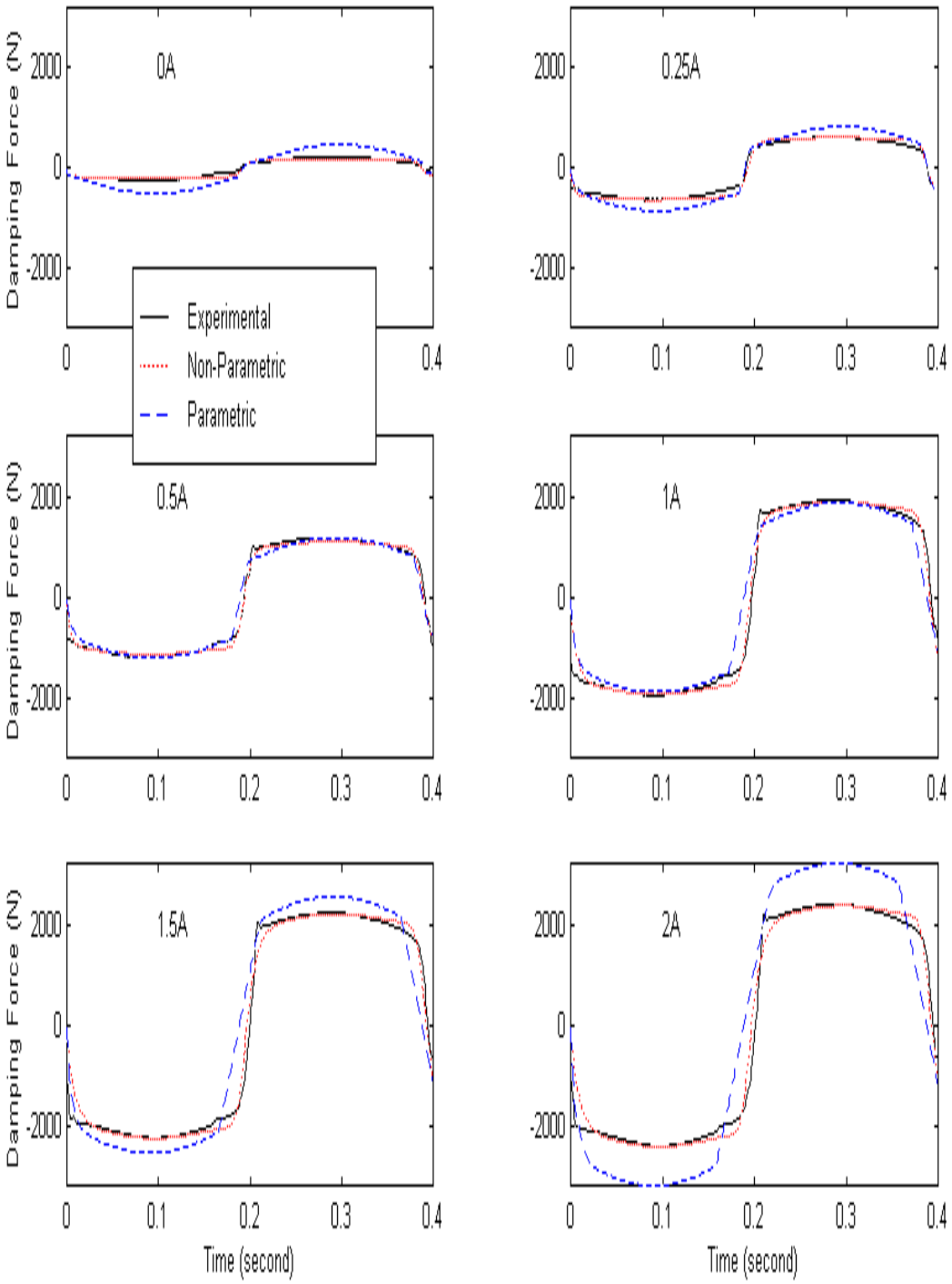

Figure 3.5 Damping Force Versus Time

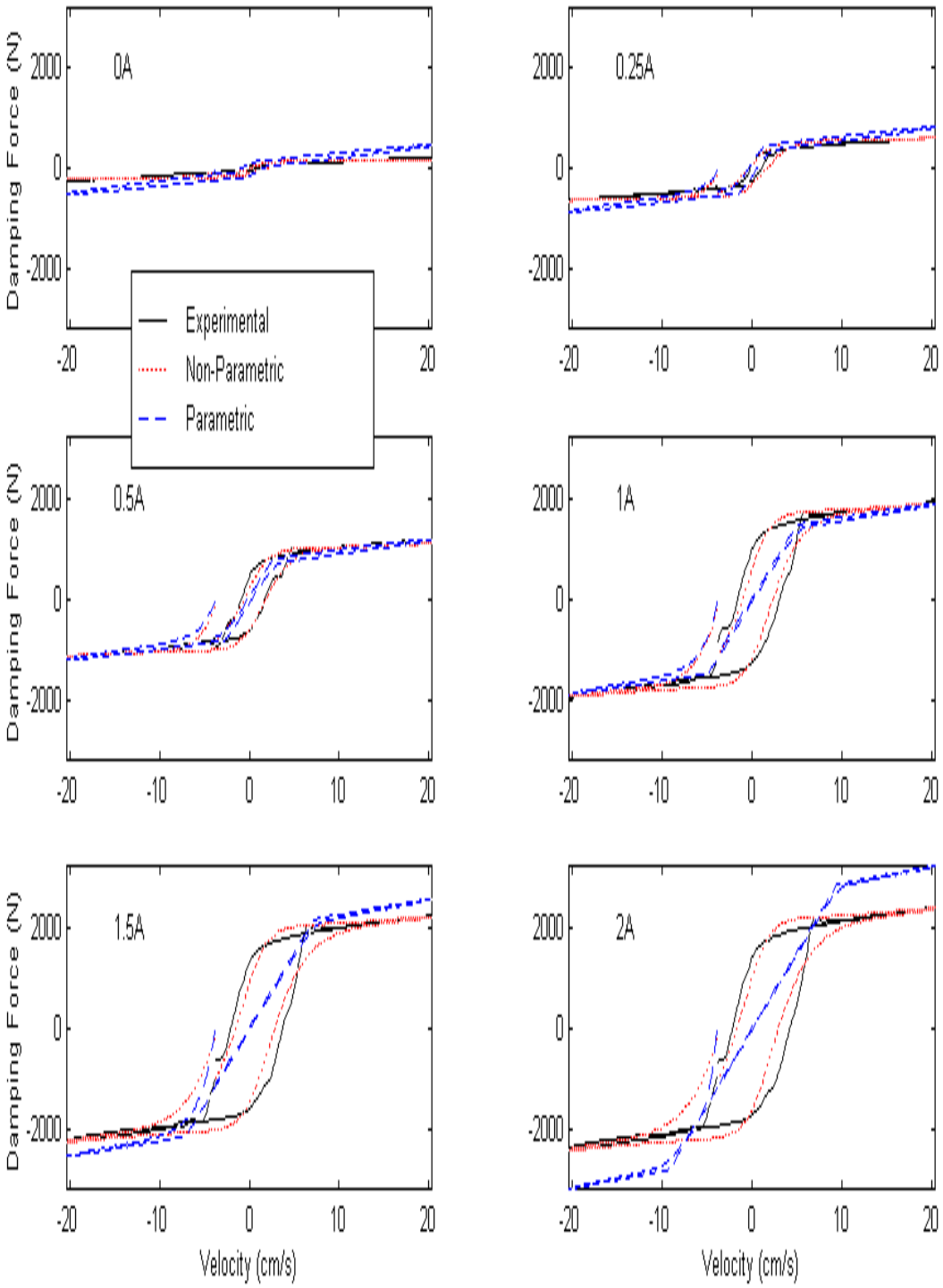

Figure 3.6 Damping Force Versus Velocity

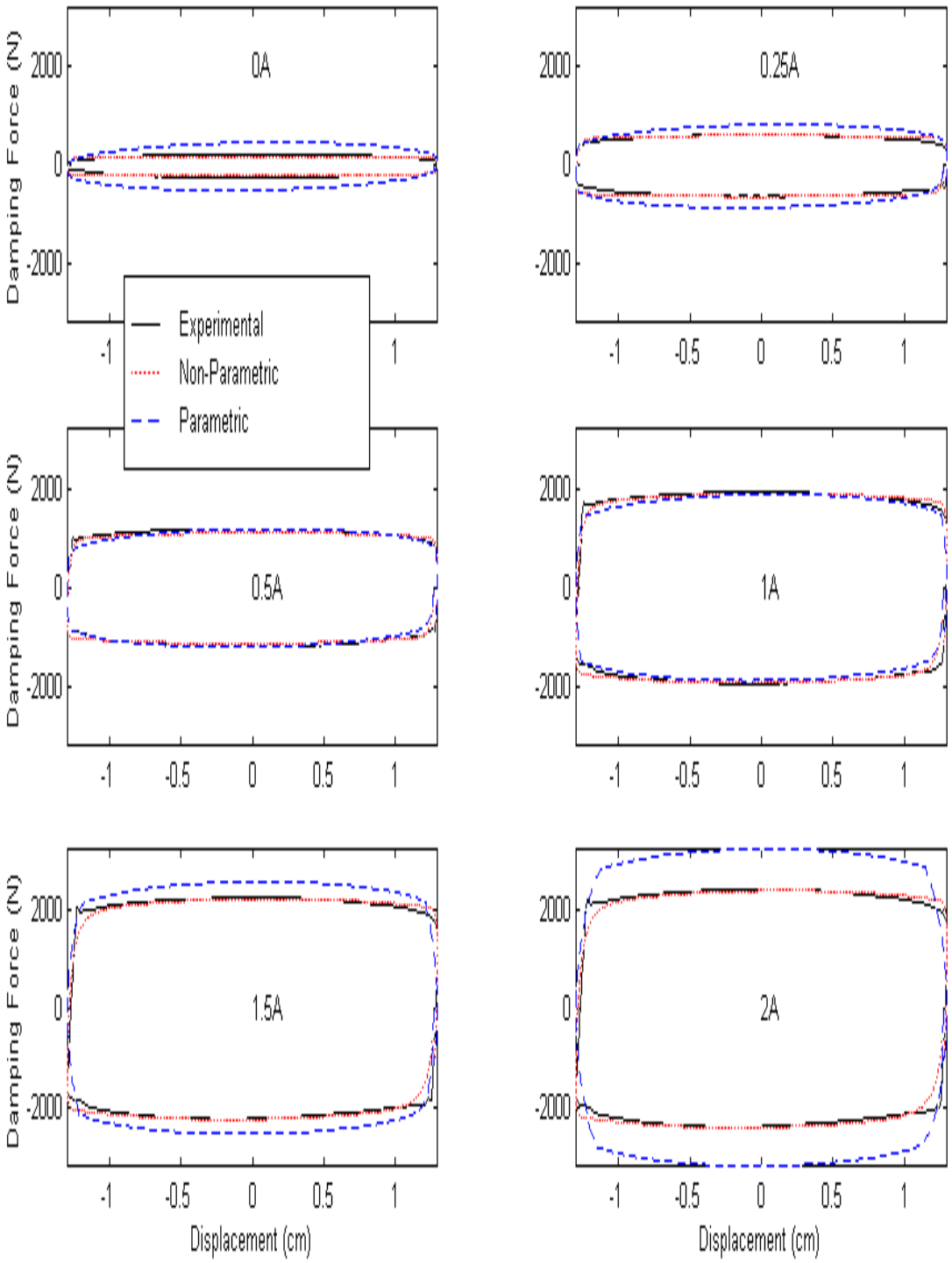

Figure 3.7 Damping Force Versus Displacement

3.6 Summary

A nonlinear non-parametric model for MR dampers was presented in this chapter. The model was configured properly to represent the physical damper characteristics, such as hysteresis and force saturation. A polynomial function was used to describe the force saturation phenomenon, and a modified hyperbolic TANH was used to capture the sharp bend in the force-velocity curve of the damper. Furthermore, a first order filter was used to represent the hysteretic behavior of the damper force.

The model results were compared with experimental data and results of a parametric model. The comparison showed that the proposed model could capture the nonlinearity of the MR damper more fully than the parametric model.

The model will be used in later chapters to develop adaptive control algorithms, and evaluate a single degree-of-freedom (DOF) dynamic system performance through simulation and experimentation. From those results shown in later chapters, it can be concluded that the non-parametric MR model works both in a quasi-static and dynamic sense.